



# Sound absorption performance of helically perforated porous metamaterials at high temperature

Weitao Zhang, Xuewei Liu, Fengxian Xin \*

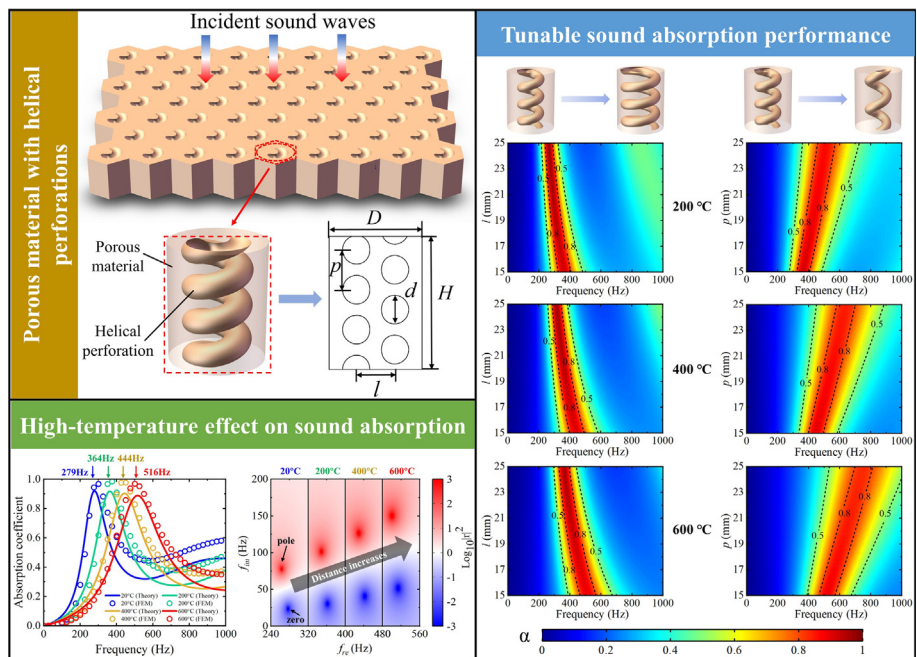
State Key Laboratory for Strength and Vibration of Mechanical Structures, Xi'an Jiaotong University, Xi'an 710049, PR China

MOE Key Laboratory for Multifunctional Materials and Structures, Xi'an Jiaotong University, Xi'an 710049, PR China

## HIGHLIGHTS

- The high-temperature sound absorption of helically perforated porous metamaterials is studied theoretically and numerically.
- An enhanced pressure diffusion effect is found in the metamaterial at relatively high frequencies at high temperature.
- The pressure diffusion effect helps to improve sound absorption performance, especially at high temperatures.
- The proposed metamaterial can be used for low-frequency sound absorption at high temperature.

## GRAPHICAL ABSTRACT



## ARTICLE INFO

### Article history:

Received 24 August 2022

Revised 22 November 2022

Accepted 26 November 2022

Available online 28 November 2022

### Keywords:

High temperature

Helically perforated porous metamaterial

Sound absorption

## ABSTRACT

A high-temperature theoretical model is established to investigate the sound absorption performance of helically perforated porous metamaterials (HPPM) at high temperature. Finite element simulations are carried out to validate the theoretical model, and good agreements have been achieved. By perforating three-dimensional helical holes in homogeneous porous material, sound waves can enter the porous material matrix more fully through these extended macroscopic helical perforations, thereby obtaining good low-frequency sound absorption at high temperatures. The results show that with the increase of temperature, the impedance matching between the metamaterial and air becomes better, so as to improve the low-frequency sound absorption ability. Compared to homogeneous porous materials, the average absorption coefficient is greatly improved, especially at higher temperatures. The numerical results of sound pressure and energy dissipation at different temperatures show that high-

\* Corresponding author.

E-mail address: fxxin@mail.xjtu.edu.cn (F. Xin).

temperature enhances the pressure diffusion effect at off-peak frequencies, resulting in more energy dissipation in high sound pressure regions. The helically perforated porous metamaterials with large helical diameter and low pitch exhibit better sound absorption performance in the low frequency range. The proposed metamaterial can be used for low-frequency sound absorption at high temperature.

© 2022 The Author(s). Published by Elsevier Ltd. This is an open access article under the CC BY-NC-ND license (<http://creativecommons.org/licenses/by-nc-nd/4.0/>).

## 1. Introduction

Porous materials are widely used for sound absorption due to their light weight, low cost and easy availability [1]. Traditional homogeneous porous materials have good sound absorption performance at high frequencies, but poor performance at low frequencies. Due to the quarter-wavelength resonance, it is difficult for porous materials to achieve ideal low-frequency sound absorption when taking into account the thickness constraints of practical use.

To overcome this problem, many artificially designed porous materials, also known as metaporous materials or porous metamaterials, have been proposed to improve the low-frequency sound absorption performance of their porous matrix without increasing thickness. Adding resonators [2–7] to porous material can bring additional absorption peaks at low frequencies. Inserting rigid plates [8–10] into porous materials helps to increase the absorption coefficient and reduce peak frequencies. The topologically designed and optimized mesoporous materials [11,12] can achieve broadband sound absorption in the mid-low frequency range. Combining air cavities [13–16] and micro-perforated panels [17–19] with porous materials is also a good way to improve the low-frequency sound absorption performance of porous materials. In addition, the multiscale design of porous materials is used to improve the low-frequency absorption capacity. Perforating porous materials with slits [20–23] and holes [24–27] allows long wavelength sound waves to enter the material and then dissipate, resulting in great subwavelength sound absorption.

The above studies mainly focus on the application at room temperature. With the development of aerospace industry, the demand for high temperature sound absorption has been increasing in recent years. Metal porous materials [28,29] and ceramic fibre materials [30] can be used for high temperature sound absorption because of their high temperature resistance. However, these traditional homogeneous porous materials exhibit poor sound absorption at low frequencies. It is of great significance to improve the low-frequency absorption performance of porous materials at high temperatures. A porous metamaterial for high-temperature sound absorption is proposed and studied [25], which is constructed by introducing cylindrical perforations into the porous material. This metamaterial has a peak frequency of 740 Hz at 500 °C and shows efficient sound absorption in the mid-low frequency range. In high temperature environment, the sound absorption of a porous metamaterial composed of macro-holes and two different porous materials was also studied [27], which showed that the sound energy dissipation of the porous materials was enhanced in low frequencies. However, it is not enough to meet diverse sound absorption requirements in high temperature environments, and deeper subwavelength sound absorbing materials are needed.

In this work, the high-temperature sound absorption performance of helically perforated porous metamaterial (HPPM) is investigated. The metamaterials constructed by perforating a porous matrix with helical macro-holes. Based on the double porosity theory and the temperature-dependent physical parameters of air, a high-temperature theoretical model is established, which is verified by numerical simulations through COMSOL Multiphysics.

High-temperature effects are explored by analyzing the sound absorption coefficient and surface impedance of the metamaterial at different temperatures. The metamaterial is compared with homogeneous porous matrix and helically perforated impervious plate to demonstrate the superiority of the porous metamaterial. To gain a deep insight into the absorption mechanism, the sound pressure and energy dissipation distributions are studied and discussed in detail. In addition, the influences of key geometric parameters on sound absorption are investigated, and the appropriate values of these parameters are explored to improve the sound absorption performance at high temperature.

## 2. Theoretical model

**Fig. 1(a)** illustrates the proposed helically perforated porous metamaterial (HPPM), which is constructed by perforating a porous material matrix with periodic helical holes. The upper surface of the metamaterial is connected to air and receives incident sound waves, while the lower surface is connected to a sound hard boundary. **Fig. 1(b)** shows an equivalent cylindrical unit cell of HPPM and the cross section of the unit cell, which shows five parameters of the structure, including unit cell height  $H$  and diameter  $D$ , helix diameter  $l$ , pitch  $p$  and hole diameter  $d$ . The incident sound waves are assumed to be normal plane harmonics. When the sound waves enter the unit cell, the propagation path in the helical hole can be equivalent to the propagation path in the oblique hole with an oblique angle  $\cos \varphi = p / \sqrt{(\pi l)^2 + p^2}$ .

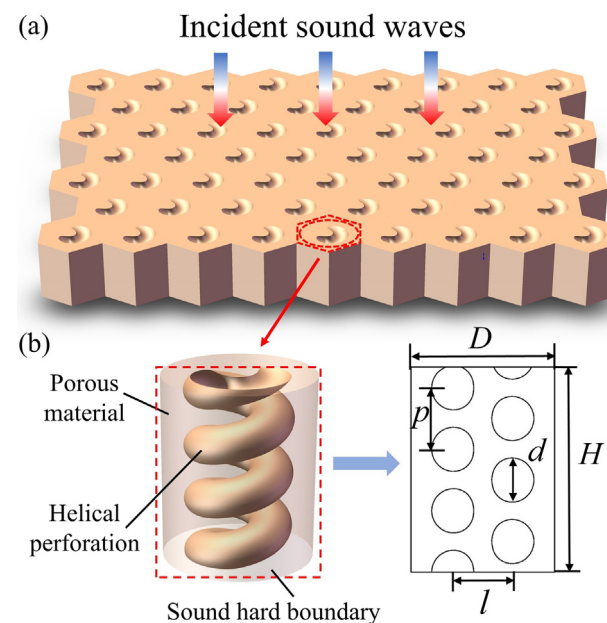


**Fig. 1.** (a) Sound propagation in a porous material matrix with periodic helical perforations; (b) Equivalent cylindrical unit cell of the helically perforated porous metamaterial (HPPM), and a cross section of the unit cell showing five geometric parameters.

Based on the double porosity theory, the perforated porous material can be regarded as a combination of the porous material matrix and the helical perforations, with its acoustic properties effective density  $\rho_{dp}$  and effective bulk modulus  $K_{dp}$  are given by [31].

$$\rho_{dp} = \left[ \rho_p^{-1} + (1 - \phi_p) \rho_m^{-1} \right]^{-1} \quad (1)$$

$$K_{dp} = \left[ K_p^{-1} + F_d(\omega)(1 - \phi_p) K_m^{-1} \right]^{-1} \quad (2)$$

The  $\rho_p$  and  $K_p$  are the effective density and bulk modulus of the helical perforation hole with the porosity  $\phi_p = d^2/(D^2 \cos \varphi)$ .  $F_d(\omega)$  is the dynamic diffusion function, which represents the ratio of the average sound pressure in the porous material to that in the helical perforation holes, and can be calculated by [20,31].

$$F_d(\omega) = 1 - \frac{j\omega P_0}{\omega_d \phi_m K_m} \left( \frac{j\omega P_0}{\omega_d \phi_m K_m} + \sqrt{1 + \frac{j\omega P_0}{\omega_d \phi_m K_m} \frac{M_d}{2}} \right)^{-1} \quad (3)$$

where  $j = \sqrt{-1}$  is the imaginary unit,  $\omega$  is the angular frequency,  $P_0 = 101325\text{Pa}$  is the atmospheric pressure.  $\phi_m$  is the porosity of the porous material matrix. The parameter  $\omega_d = (1 - \phi_p)P_0/[\phi_m \sigma_m D(0)]$  is the characteristic frequency representing the pressure diffusion effect, where  $D(0) = (1 - \phi_p)\pi D^2/4$  is the static pressure permeability. The parameter  $M_d = 8D(0)/[\Lambda_d^2(1 - \phi_p)]$  is related to  $\Lambda_d = 2\Omega_m/\Gamma_{mp}$ , and is defined as twice the ratio of the volume of porous material domain  $\Omega_m = \pi D^2 H(1 - \phi_p)/4$  to the interfacial area between the porous material domain and air  $\Gamma_{mp} = (\pi D^2 - \pi d^2/\cos \varphi)/4 + \pi dH/\cos \varphi$ .

For the porous material matrix, the Johnson-Champoux-Allard (JCA) model is used to describe its acoustic properties. The effective density  $\rho_m$  and the effective bulk modulus  $K_m$  are given by [23,32].

$$\rho_m = \frac{\alpha_{\infty m} \rho_0}{\phi_m} \left( 1 + \frac{\phi_m \sigma_m}{j\omega \rho_0 \alpha_{\infty m}} \sqrt{1 + j \frac{4\omega \eta \rho_0 \alpha_{\infty m}^2}{\sigma_m^2 \Lambda_m^2 \phi_m^2}} \right) \quad (4)$$

$$K_m = \frac{\gamma P_0}{\phi_m} \left[ \gamma - (\gamma - 1) \left( 1 - j \frac{8\kappa}{\omega \rho_0 C_p \Lambda_m^2} \sqrt{1 + j \frac{\omega \rho_0 C_p \Lambda_m^2}{16\kappa}} \right)^{-1} \right]^{-1} \quad (5)$$

where the tortuosity  $\alpha_{\infty m}$ , porosity  $\phi_m$ , static flow resistivity  $\sigma_m$ , viscous characteristic length  $\Lambda_m$  and thermal characteristic length  $\Lambda'_m$  are the parameters of the porous material matrix. The parameter  $\rho_0$  is density,  $\eta$  is dynamic viscosity,  $\gamma$  is heat ratio,  $\kappa$  is thermal conductivity,  $C_p$  is specific heat capacity of air.

For the helical perforation hole, the effective density  $\rho_p$  and the effective bulk modulus  $K_p$  are given by [27,32].

$$\rho_p = \frac{\alpha_{\infty p} \rho_0}{\phi_p} \left[ 1 - \frac{2}{\beta \sqrt{-j}} \frac{J_1(\beta \sqrt{-j})}{J_0(\beta \sqrt{-j})} \right]^{-1} \quad (6)$$

$$K_p = \frac{\gamma P_0}{\phi_p} \left[ 1 + (\gamma - 1) \frac{2}{\beta \sqrt{-j} \Pr} \frac{J_1(\beta \sqrt{-j} \Pr)}{J_0(\beta \sqrt{-j} \Pr)} \right]^{-1} \quad (7)$$

where  $\alpha_{\infty p} = 1/\cos^2 \varphi$  is the tortuosity of the helical perforation,  $\beta = d\sqrt{\omega \rho_0 / \eta} / 2$  with  $\Pr = \eta C_p / \kappa$  being the Prandtl number, and  $J_0(\cdot)$  and  $J_1(\cdot)$  are the zero-order and first-order Bessel functions, respectively.

After combining the two parts according to Eqs. (1) and (2), the acoustic wavenumber and the characteristic impedance of the

metamaterial can be calculated by  $Z_{dp} = \sqrt{\rho_{dp} K_{dp}}$  and  $k_{dp} = \omega \sqrt{\rho_{dp} / K_{dp}}$ , respectively. Then the surface impedance  $Z_s$  and sound absorption coefficient  $\alpha$  can be obtained by.

$$Z_s = -j Z_{dp} \cot(k_{dp} H) \quad (8)$$

$$\alpha = \frac{4 \operatorname{Re}(Z_s) / Z_0}{[1 + \operatorname{Re}(Z_s) / Z_0]^2 + [\operatorname{Im}(Z_s) / Z_0]^2} \quad (9)$$

where  $\operatorname{Re}(\cdot)$  and  $\operatorname{Im}(\cdot)$  represent the real part and imaginary part,  $Z_0 = \rho_0 c_0$  is the characteristic impedance of air, and  $c_0$  is the sound speed of air.

To explore the sound absorption performance at high temperatures, the temperature-dependent physical parameters of air should be considered in the theoretical model. With the increase of temperature, several physical parameters of air will change significantly. Here, the application environment of the metamaterial is considered as an open thermal system. Although a high temperature environment is considered, the system always remains isobaric at standard atmospheric pressure and the molecular mean free path is large enough to reduce the interactions between air molecules. Therefore, the ideal gas law remains valid. Then the temperature dependence of the air mass density is isobaric and can be accurately predicted using the ideal gas law as.

$$\rho_0 = \frac{P_0}{R_s T} \quad (10)$$

where  $R_s = 286.987 \text{ J}/(\text{K} \cdot \text{kg})$  is the specific gas constant. The sound speed can be expressed as.

$$c_0 = \sqrt{\gamma R_s T} \quad (11)$$

The dynamic viscosity of air is a key parameter controlling viscous dissipation, having a relationship with  $T$  as [33].

$$\eta = \eta_0 \left( \frac{T}{T_0} \right)^{1.5} \left( \frac{C_s + T_0}{C_s + T} \right) \quad (12)$$

Where  $C_s = 120\text{K}$ ,  $T_0$  is the reference temperature,  $\eta_0$  is the value of  $\eta$  at  $T_0$ .

The air thermal conductivity and specific heat capacity related to thermal dissipation will also change with the increase of temperature. In COMSOL multiphysics, their relationships with temperature have been given in the following numerical forms [25,33].

$$\kappa = \sum_{n=0}^4 (A_n \cdot T^n) \quad (13)$$

$$C_p = \sum_{n=0}^4 (B_n \cdot T^n) \quad (14)$$

where the fitting parameters  $A_n$  and  $B_n$  are listed in Table 1.

In addition, the static flow resistivity of the porous material matrix  $\sigma_m$  also changes when the dynamic viscosity is affected by temperature. It is approximately related to temperature as [34].

**Table 1**  
Values of the fitting parameters  $A_n$  and  $B_n$ .

$A_n$	Values[W/m/K <sup>n+1</sup> ]	$B_n$	Values[J/kg/K <sup>n+1</sup> ]
$A_0$	-0.00227583562	$B_0$	1047.63657
$A_1$	$1.15480022 \times 10^{-4}$	$B_1$	-0.372589265
$A_2$	$-7.90252856 \times 10^{-8}$	$B_2$	$9.45304214 \times 10^{-4}$
$A_3$	$4.11702505 \times 10^{-11}$	$B_3$	$-6.02409443 \times 10^{-7}$
$A_4$	$-7.43864331 \times 10^{-15}$	$B_4$	$1.2858961 \times 10^{-10}$

$$\sigma_m = \sigma_0 \left( \frac{T}{T_0} \right)^{0.6} \quad (15)$$

where  $\sigma_0$  is the static flow resistivity at the reference temperature  $T_0$ . As for other parameters, their changes are small and can be ignored in the model. In the above discussion, the standard atmospheric pressure  $P_0$  is fixed at 101325 Pa, and the specific heat ratio of air  $\gamma$  is fixed at 1.4. The temperature dependence of the above parameters is valid in the considered temperature range (from 20 °C to 600 °C). For the physical parameters of air, the temperature dependence can be accurately predicted by Eqs. (10)-(14) below 600 °C [28,35]. For the static flow resistivity of porous materials, the relationship in Eq. (15) will remain valid below 600 °C when the mechanical properties of porous materials remain stable at such high temperatures [36].

### 3. Results and discussion

To validate the theoretical model and further explore the sound absorption mechanism, a three-dimensional (3D) finite element model is established in COMSOL Multiphysics using the Pressure Acoustics Module, as shown in Fig. 2. The blue areas are the air domain, while the yellow area represents the porous matrix of the HPPM, which is set as the poroacoustic domain using the JCA model. The background pressure field is constructed to provide normal incident plane waves with pressure amplitude of 1 Pa. And a perfectly matched layer is established to simulate a non-reflective boundary. All walls of the 3D model are set to sound hard boundaries. To simulate a high temperature environment, the built-in temperature in the software is set to the value we are interested in, and the temperature-related parameters will change accordingly.

The parameters of the unit cell are defined as height  $H = 50$  mm, diameter  $D = 35$  mm, helix diameter  $l = 15$  mm, pitch  $p = 15$  mm and hole diameter  $d = 10$  mm. For porous matrix, polyurethane foams with relatively low decomposition temperatures and melting point, and glass fiber materials with low glass transition temperature are not suitable for high-temperature sound absorption. Metal fibers usually have stable thermal and mechanical behavior at high temperatures [37,38], and are good materials for high-temperature sound absorption. In this work, a metal-based fibrous material made of FeCrAl alloy fibers is selected as the porous matrix with five JCA parameters: porosity  $\phi_m = 0.9$ , tortuosity  $\alpha_{\infty m} = 1.05$ , viscous characteristic length  $\Lambda_m = 19.7 \mu\text{m}$ , thermal characteristic length  $\Lambda'_m = 36+$  and static flow resistivity  $\sigma_m = 489336 \text{ N} \cdot \text{s/m}^4$  at 20 °C [39].

#### 3.1. Sound absorption performance

The theoretical predictions of sound absorption coefficient and surface impedance of the helically perforated porous metamaterial (HPPM) at different temperatures (20 °C, 200 °C, 400 °C and 600 °C)

are compared with the numerical results in Fig. 3. For the results at 200 °C, good agreement is achieved in the low frequency range (below 500 Hz). The theoretical and numerical results maintain a consistent trend with increasing frequency, but the deviation between them increases slightly. This is because the theoretical model considers the pressure diffusion effect in this metamaterial in the whole frequency range. While this effect mainly occurs at low frequencies in the numerical model. As the frequency increases, the effect becomes weaker, slightly reducing the accuracy of the theoretical predictions. However, comparing the results at different temperatures, it can be seen that the deviation is reduced when increasing temperature. This is mainly because the increase of temperature will enhance the pressure diffusion effect at high frequencies (from 500 Hz to 1000 Hz). Pressure diffusion refers to the entry of sound waves from macro-perforations into micro-pores of porous materials under the effect of pressure gradient. We previously studied the effect of high-temperature on the sound absorption of cylindrically perforated porous materials, and analyzed the energy dissipation and sound intensity flow direction in porous materials at different temperatures [25]. The results show that the coupling resonance between the cylindrical perforation and porous material at high frequencies increases with the increase of temperature. Compared with the results at 20 °C, at relatively high frequencies, more sound energy can enter the porous material from the perforation hole, and more energy dissipation occurs at the interface between the perforation hole and the porous material at 500 °C. These results suggest that the pressure diffusion effect at high frequencies can be enhanced by increasing the temperature.

The HPPM is also a perforated porous metamaterial, which exhibits similar characteristics at high temperatures. This phenomenon can be explained from the perspective of sound propagation. As temperature rises, the viscous and thermal effects in micro-pores are enhanced due to the increase of the thickness of viscous and thermal layers [25]. The acoustic resistance of these micro-pores can be increased by the enhanced viscous and thermal effect, which makes it more difficult for sound waves to directly enter the porous domain. Most of the sound waves then directly enter the macroscale helical perforations, which leads to an increased sound pressure gradient at the interface between the helical perforations and the porous material. With the increased sound pressure gradient, more sound waves can enter the porous material from the helical perforations. Therefore, the pressure diffusion effect in HPPM is enhanced, and the theoretical model shows more accurate prediction ability at high temperature.

As shown in Fig. 3(a), with the increase of temperature, the sound absorption peak frequencies of the HPPM are 279 Hz, 364 Hz, 444 Hz and 516 Hz at 20 °C, 200 °C, 400 °C and 600 °C, respectively, showing an increasing trend. According to Eq. (11), the sound speed of the air in the helical perforations increases with the increase of temperature. For the air-saturated porous metamaterial, the effective sound speed also increases with the increase of temperature. The sound absorption peak occurs at the frequency where the thickness of the HPPM is equal to one-quarter wave-

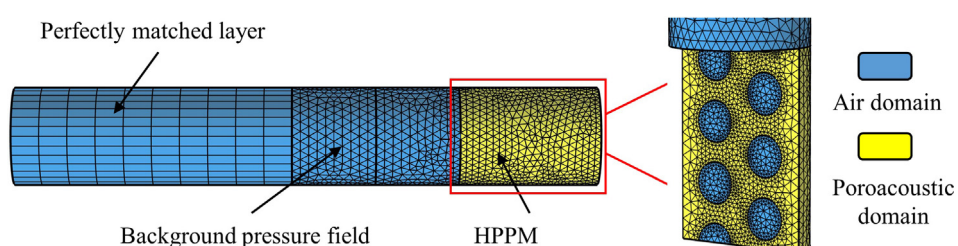


**Fig. 2.** Schematic diagram of a three dimensional finite element model for studying the sound absorption performance of the HPPM.

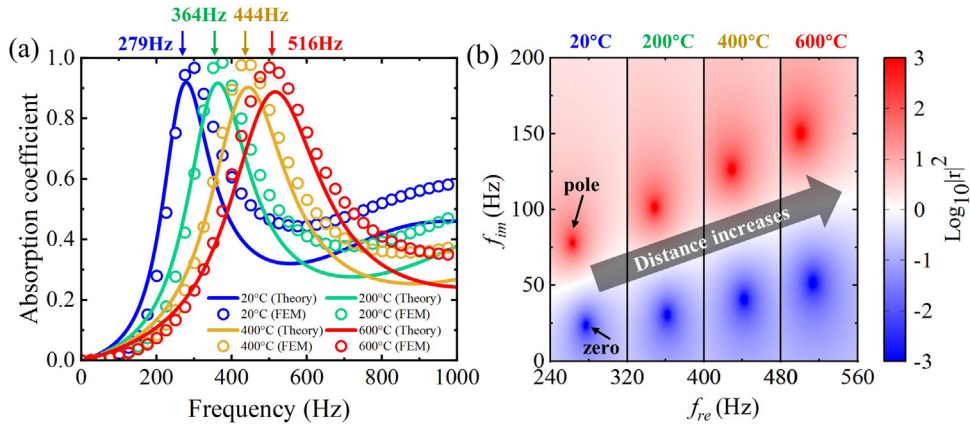


**Fig. 3.** (a) Sound absorption coefficient of the helically perforated porous metamaterial (HPPM) at different temperatures (20 °C, 200 °C, 400 °C and 600 °C). (b) Complex frequency plane description of the reflection coefficient of the HPPM at different temperatures.

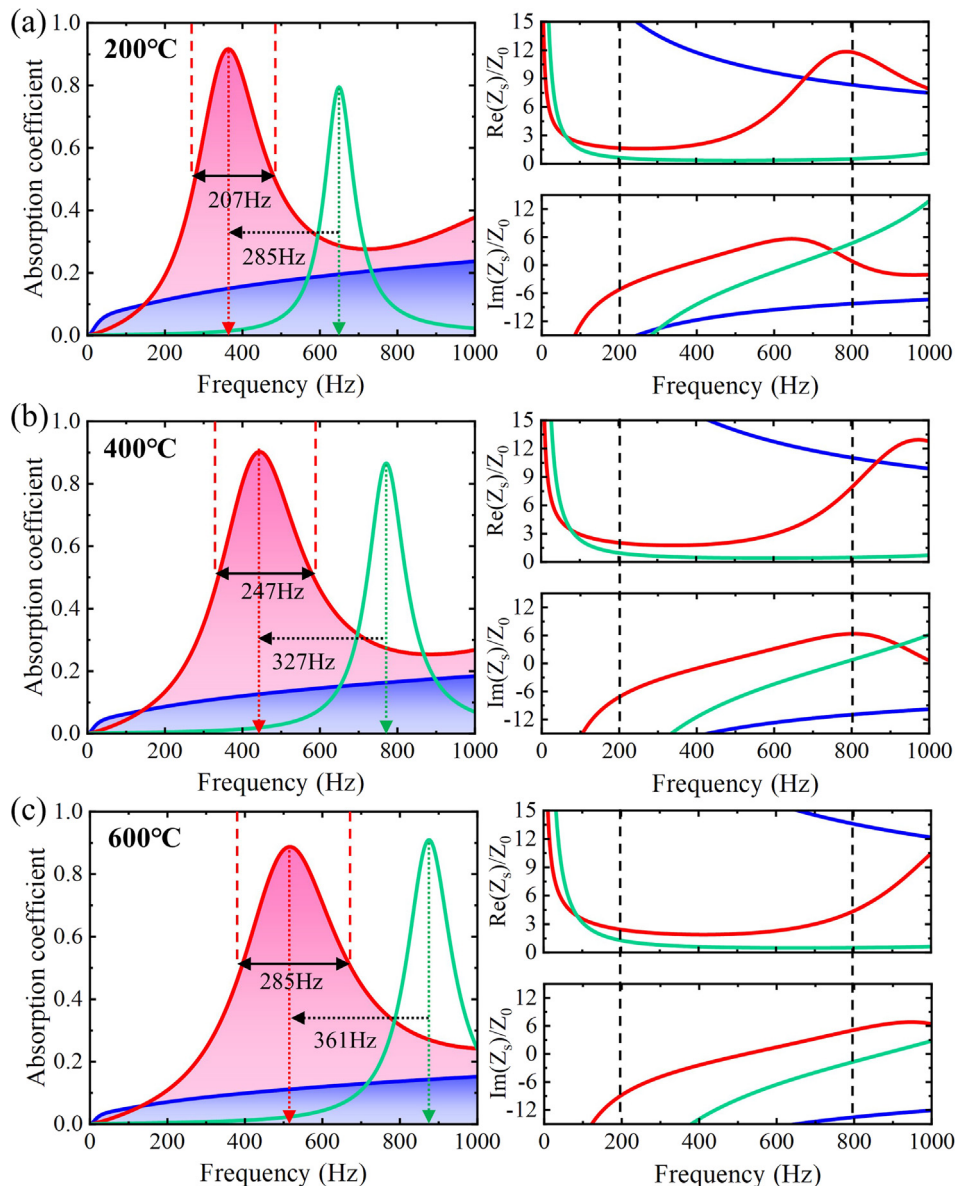


**Fig. 4.** Variation of sound absorption coefficient and normalized surface impedance with frequency at different temperatures: (a) 200 °C; (b) 400 °C; (c) 600 °C. Red lines are related to helically perforated porous metamaterial (HPPM), blue lines are related to homogeneous porous material, and green lines are related to helically perforated impervious plate (HPIP).

length of the sound waves. Since the thickness of the HPPM remains unchanged, the wavelength of the sound waves also remains unchanged when resonance occurs. Therefore, with the increase of temperature, a higher resonance frequency is required due to the increase in sound speed according to the relationship  $\lambda = c/f$  between sound speed  $c$  and wavelength  $\lambda$ , so as to push up the absorption peak frequency of the HPPM.

Compared with the sound absorption performance at 20 °C, the half-absorption bandwidth of the HPPM shows a wider trend with the increase of temperature, as shown in Fig. 3(a). To illustrate this phenomenon and further explore the effect of high temperature on sound absorption, the complex frequency plane description of the reflection coefficient of the HPPM at different temperatures is analyzed here. The frequency is decomposed as  $f = f_{re} + jf_{im}$ , then the description of the reflection coefficient can be expressed as a function of the real frequency  $f_{re}$  and the imaginary frequency  $f_{im}$ . At 20 °C, the zero and pole points of the reflection coefficient are located above the real frequency axis, indicating the over damping state of the HPPM. With the increase of temperature, both the zero and pole points move forward along the imaginary frequency axis, resulting in an enhanced over damping state of the HPPM. This indicates that high-temperature can increase the damping and energy loss capability of the porous metamaterial. The distance between the zero and pole points is related to the bandwidth of the absorber. As shown in Fig. 3(b), the distance between zero and pole points increases with the increase of temperature from 20 °C to 600 °C, thus broadening the half-absorption bandwidth of the HPPM.

It can also be found from Fig. 3(a) that the sound absorption coefficient of the theoretical results is lower than the numerical

results at the peak frequency. This is precisely because the viscosity is considered in the theoretical model, while it is not considered in the numerical calculation. According to the complex frequency plane analysis, the considered HPPM belongs to the over damping state, as shown in Fig. 3(b). In the over damping state, increasing the energy loss of the system will enhance the damping state, and the enhancement of the over damping state will lead to the deterioration of sound absorption performance. Or in other words, the over-damped state means that the material has a large acoustic impedance and a large mismatch with the air impedance, which will reduce the sound absorption coefficient. Therefore, the theoretical model predicts a decrease in the absorption coefficient at the peak frequency.

For comparison, the sound absorption and surface impedance of homogeneous porous material matrix of the HPPM at different temperatures are plotted in Fig. 4(a)-(c). The blue areas represent the sound absorption performance of the porous material matrix, while the pink areas represent the enhanced sound absorption coefficient of the HPPM compared to its porous material matrix. When sound waves propagate from air into sound absorbers, appropriate impedance matching condition can induce effective sound absorption. According to Eq. (9), a high value of  $\alpha$  occurs when the real part of the surface impedance normalized by the air characteristic impedance reaches 1 and the imaginary part reaches 0. From these figures, it can be seen that as the temperature increases, the sound absorption performance of the porous material deteriorates due to the increase of sound resistance (real part of surface impedance) and the decrease of sound reactance (imaginary part of surface impedance). After perforating periodic helical holes in the porous material, the low-frequency sound

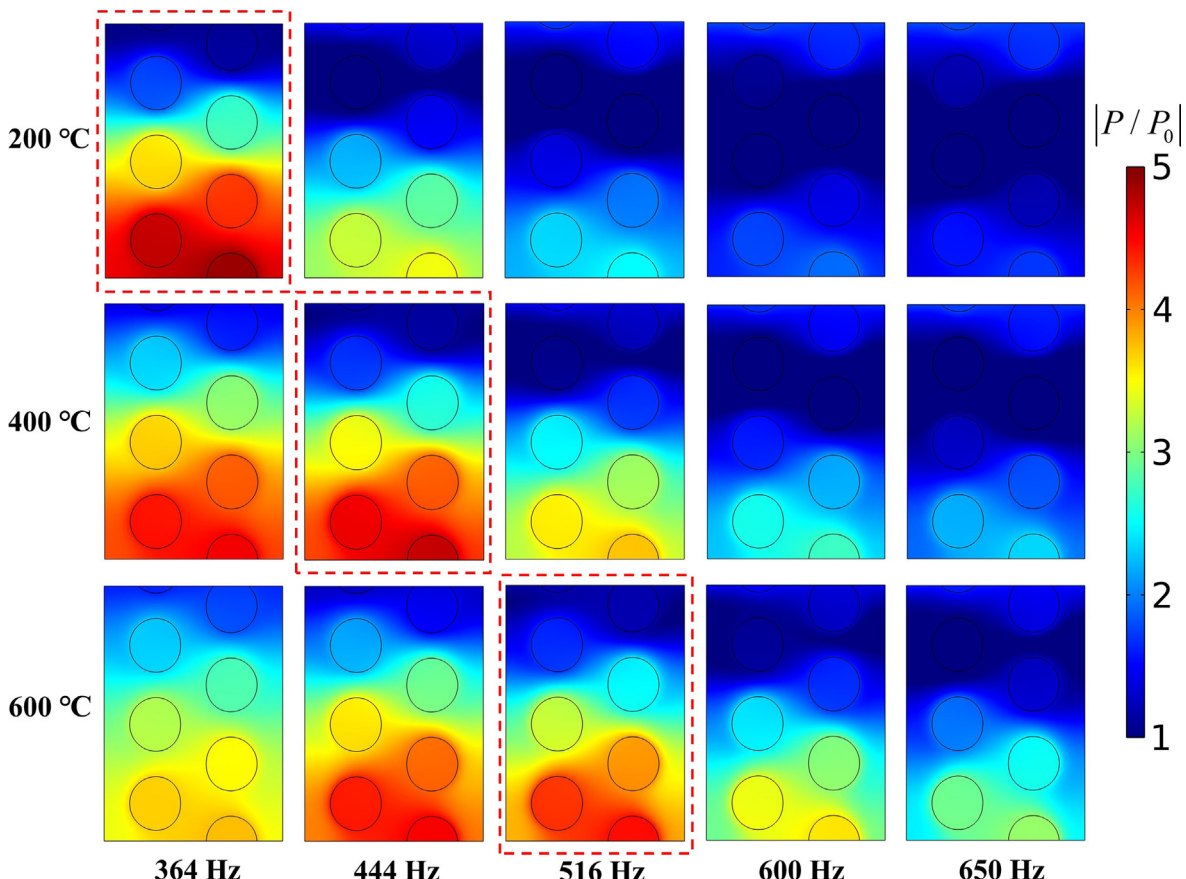


**Fig. 5.** Sound pressure distributions of the unit cell cross-section at different frequencies (364 Hz, 444 Hz, 516 Hz, 600 Hz and 650 Hz) and different temperatures (200 °C, 400 °C and 600 °C).  $P_0$  is the amplitude of incident sound waves.

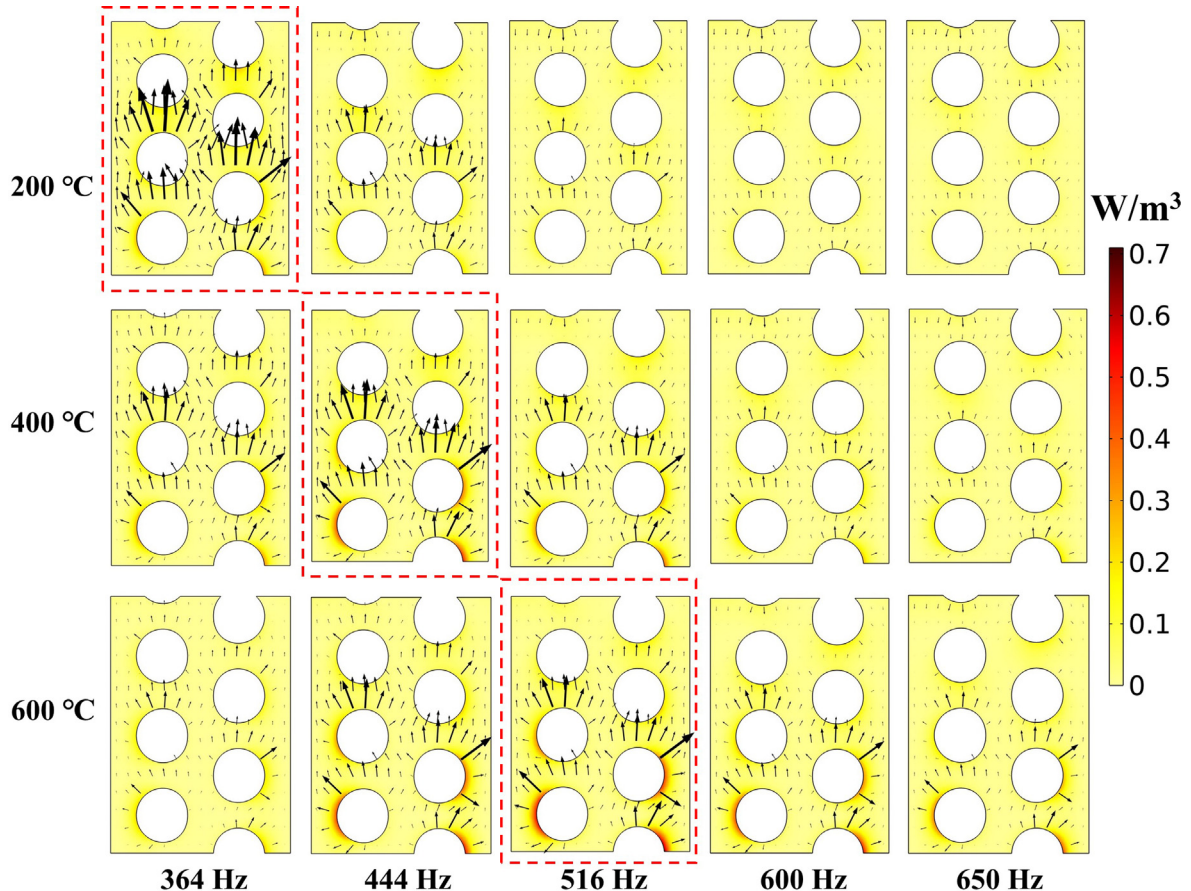


**Fig. 6.** Sound energy dissipation density ( $\text{W}/\text{m}^3$ ) and sound intensity flows of the unit cell cross-section at different frequencies (364 Hz, 444 Hz, 516 Hz, 600 Hz and 650 Hz) and different temperatures (200 °C, 400 °C and 600 °C).

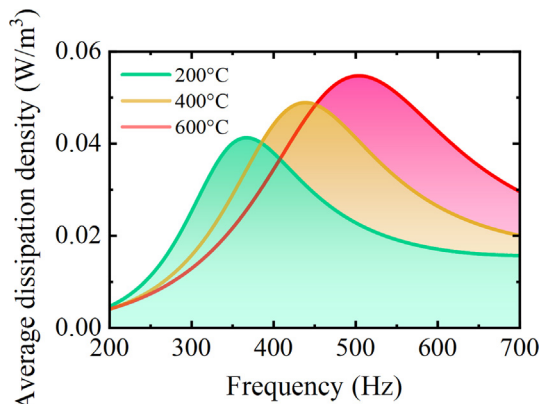


**Fig. 7.** Average sound energy dissipation density ( $\text{W}/\text{m}^3$ ) in porous material as a function of frequency at different temperatures (200 °C, 400 °C and 600 °C).

absorption capacity is greatly enhanced, and it becomes more stable at high temperature. Compared with the homogeneous porous material matrix, the average sound absorption coefficient of the HPPM can reach 184 %, 287 % and 389 % at 200 °C, 400 °C and 600 °C, respectively, showing superior low-frequency sound absorption at high temperatures. From the perspective of impedance matching, the impedance matching between the porous material and air is improved, which greatly enhances low-frequency sound absorption, especially at high temperatures.

Since the wall of the helical perforation is made of porous material, which is permeable to sound waves, the pressure diffusion effect between the perforation and porous material plays an important role in sound absorption. To investigate the influence of the pressure diffusion effect, Fig. 4(a)-(c) compare the sound absorption coefficients of helically perforated porous metamaterial (HPPM) and helically perforated impervious plate (HPIP) at different temperatures. For the results at 200 °C, the sound absorption of HPPM is greatly enhanced at low frequencies compared to HPIP. This is because the propagation path of sound waves is different in these two materials. In HPIP, the sound waves can only propagate along the helical hole because the wall of the perforation is impervious. In HPPM, the sound waves not only propagate along the helical hole, but also can enter the porous material under the pressure diffusion effect, resulting in a longer propagation path and lower absorption peak in the metamaterial. As the temperature rises, HPPM reduces the peak frequency of HPIP at 200 °C, 400 °C and 600 °C by 285 Hz, 327 Hz and 361 Hz, respectively, showing more stable low-frequency sound absorption when the temperature increased. Meanwhile, it can be seen from Fig. 4 that the bandwidth of HPPM is significantly larger than that of HPIP, indicating that the pressure diffusion effect plays a role in favor of dissipating sound energy in a wider frequency range.

To see the pressure diffusion effect in the HPPM clearly, Fig. 5 illustrates the sound pressure distributions of the unit cell cross-section at different frequencies (364 Hz, 444 Hz, 516 Hz, 600 Hz and 650 Hz) and different temperatures (200 °C, 400 °C and 600 °C). Here, 364 Hz, 444 Hz, and 516 Hz are peak frequencies at 200 °C, 400 °C and 600 °C respectively, while 600 Hz and

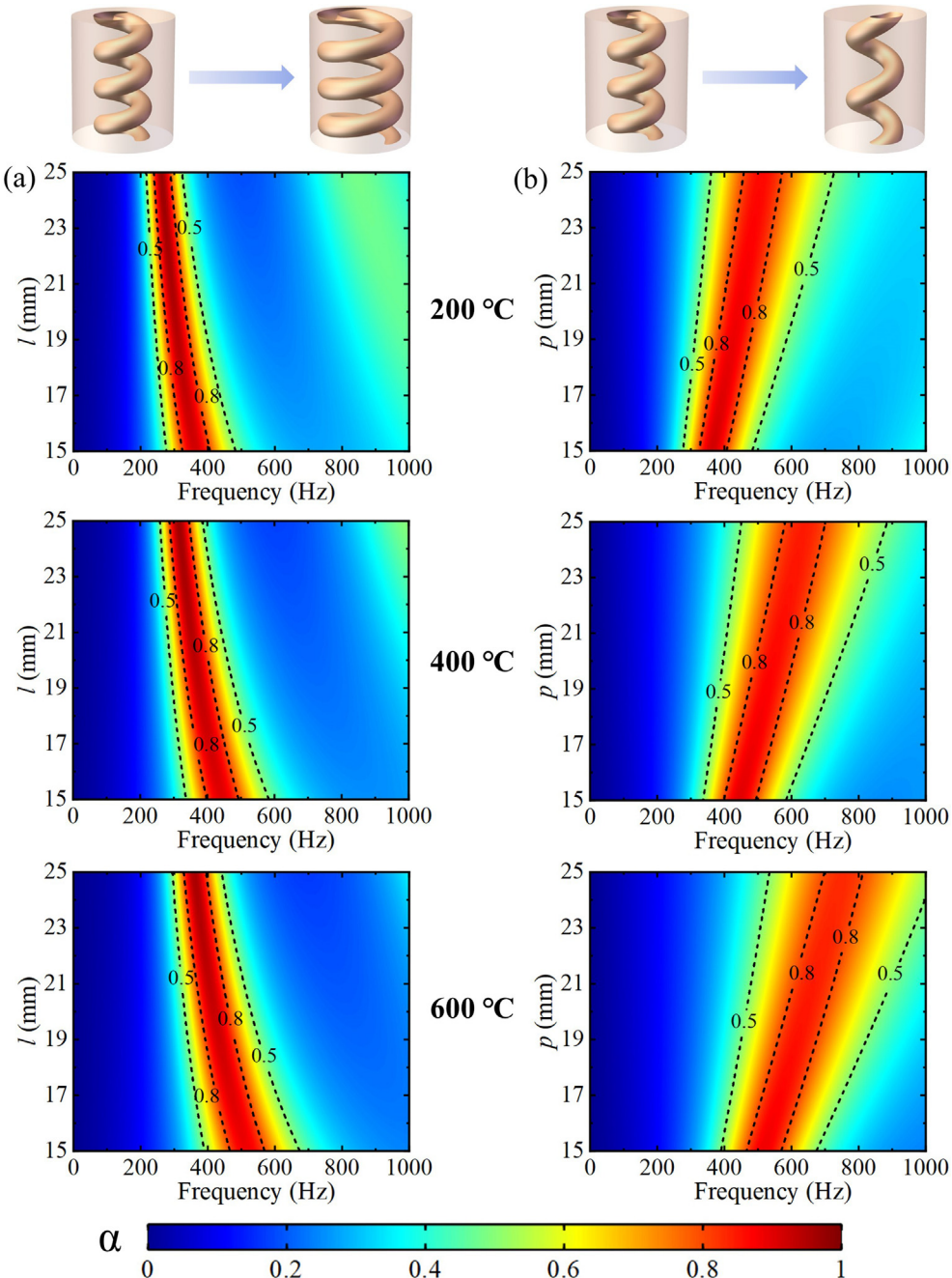


**Fig. 8.** Sound absorption of HPPM at different temperatures ( $200\text{ }^{\circ}\text{C}$ ,  $400\text{ }^{\circ}\text{C}$  and  $600\text{ }^{\circ}\text{C}$ ): (a) influence of the helical perforation diameter; (b) influence of the helical perforation pitch.

650 Hz are two reference frequencies. It can be seen from Fig. 5 that the high sound pressure mainly appears at the bottom of the metamaterial, because the micro-pore size of the porous material is too small, and the sound waves of large wavelength cannot directly enter. Therefore, the incident sound waves first reach the bottom through the helical perforation hole and are reflected by the rigid back, and then standing waves appear due to the interference of the incident and reflected sound waves. The increased sound pressure in the macro-holes leads to a non-uniform distribution, which means that there is a pressure gradient between the helical hole and the porous material, resulting in pressure diffusion effect. The non-uniform distribution is more obvious near the peak frequency, indicating that the pressure diffusion effect plays an important role in sound absorption. With the increase of tempera-

ture, the inhomogeneity of the pressure distribution at these selected frequencies becomes more pronounced, especially at high frequencies, which means that the pressure diffusion effect is enhanced and can work over a wider frequency range. Therefore, the HPPM exhibits better sound absorption performance at high temperatures.

To gain a deeper insight into the sound absorption mechanism, the sound energy dissipation and sound intensity flow of the unit cell cross-section at different temperatures are illustrated in Fig. 6. The colors represent the energy dissipation density (unit:  $\text{W}/\text{m}^3$ ), and the arrows represent the vector sound intensity flow. Of the five frequencies selected, 364 Hz, 444 Hz, and 516 Hz are the absorption peak frequencies at  $200\text{ }^{\circ}\text{C}$ ,  $400\text{ }^{\circ}\text{C}$  and  $600\text{ }^{\circ}\text{C}$ , respectively. For the results at a certain temperature, the sound

energy mainly propagates from the helical holes to the porous material under the pressure diffusion effect, and then dissipates through viscosity and thermal conduction in the porous material. The energy dissipation near the interface between the helical hole and the porous material is significantly higher than in other regions. Combining with Fig. 5 and Fig. 6, it can be seen that the high energy dissipation region is also a high sound pressure region. In these regions, the contrast between the sound pressure in the helical hole and the porous material is more pronounced, which can enhance the sound energy dissipation. And as the temperature increases, the dissipation also increases significantly. At 200 °C, 400 °C, and 600 °C, the maximum energy dissipation densities of the selected cross-section are 0.33 W/m<sup>3</sup>, 0.54 W/m<sup>3</sup> and 0.68 W/m<sup>3</sup>, respectively. The average dissipation densities of porous material at different temperatures are also calculated numerically, as shown in Fig. 7. Comparing the results at different temperatures, not only the energy dissipation at peak frequency increases, but also the dissipation near the peak frequency increases significantly, resulting in a wider half-absorption bandwidth of the HPPM, as shown in Fig. 3.

### 3.2. Influence of geometric parameters

The sound absorption performance of the HPPM is affected by its geometric parameters, especially the helix diameter  $l$  and the pitch  $p$  of the helical perforation. Fig. 8(a) shows the influence of the helix diameter on sound absorption coefficient at 200 °C, 400 °C and 600 °C, respectively, where the warm colors indicate high values (0.5–1) and the cool colors indicate low values (0–0.5). For the results at a certain temperature, the peak value of the sound absorption coefficient will increase, and the peak frequency will decrease with the helix diameter  $l$  increases, which means that the low-frequency sound absorption performance becomes better. This mainly because the sound propagation path in the helical hole is prolonged with increasing the helix diameter  $l$ , which makes the resonance occur at lower frequencies. At 200 °C, the HPPM designed with  $l = 15$  mm reaches its peak absorption at 364 Hz, while 516 Hz at 600 °C, the peak frequency is increased by 157 Hz due to the increased temperature. For the HPPM with  $l = 25$  mm, the peak frequency increases by 88 Hz, indicating that the HPPM with large helical diameter has more stable low-frequency absorption capacity in the face of temperature changes.

Fig. 8(b) illustrates the influence of the pitch at different temperatures. Different from the influence of the helical diameter, it can be seen that with the increase of the pitch, the peak absorption coefficient decreases and the peak frequency increases. As the three dimensional models shown in Fig. 8(b), increasing the pitch can greatly reduce the tortuosity of the helical hole, and then the sound absorption performance deteriorates in the low frequency range. At 200 °C, when the pitch increases from 15 mm to 25 mm, the peak frequency varies from 364 Hz to 516 Hz, while at 600 °C the peak frequency varies from 513 Hz to 755 Hz, indicating that low-frequency sound absorption capacity of small pitch HPPM is more stable at high temperatures.

### 4. Concluding remarks

In this work, the sound absorption performance of the helically perforated porous metamaterials (HPPM) at high temperatures (200 °C, 400 °C and 600 °C) are studied theoretically and numerically. As the temperature increases, the resonance is delayed in the frequency domain, and the absorption peak moves to a higher frequency. The analysis of impedance matching shows that high temperature can improve the low-frequency matching conditions,

and then broaden the half-absorption of the HPPM. The numerical results of sound pressure and energy dissipation density distributions help to reveal the sound absorption mechanism at different temperatures. With the increase of temperature, the pressure diffusion effect at off-peak frequencies is enhanced, which means that it can work in a wider frequency range. With an increased pressure gradient between the helical pores and the porous material, more sound energy can enter the porous domain and then dissipate at higher temperatures, resulting in better sound absorption performance. The diameter and pitch of the helical perforation are two key geometric parameters, which can affect sound absorption performance by altering the tortuosity and sound propagation path of the helical perforation. The influences of these two parameters on sound absorption at different temperatures are explored. The results show that the HPPM with large helix diameter and small pitch has more stable low-frequency sound absorption performance when the temperature increases. This work can provide guidance for the design and optimization of porous metamaterials to meet the requirements of low-frequency sound absorption in high temperature environments.

### 5. Data availability

The data that support the findings of this study are available from the corresponding author upon reasonable request.

#### Data availability

Data will be made available on request.

#### Declaration of Competing Interest

The authors declare that they have no known competing financial interests or personal relationships that could have appeared to influence the work reported in this paper.

#### Acknowledgements

This work was supported by the National Natural Science Foundation of China (52075416, 11772248 and 11761131003) and the Fundamental Research Funds for the Central Universities (LX6J013).

#### References

- [1] L. Cao, Q. Fu, Y. Si, B. Ding, J. Yu, Porous materials for sound absorption, Compos. Commun. 10 (2018) 25–35.
- [2] J.P. Groby, C. Lagarrigue, B. Brouard, O. Dazel, V. Tournat, B. Nennig, Enhancing the absorption properties of acoustic porous plates by periodically embedding Helmholtz resonators, J. Acoust. Soc. Am. 137 (1) (2015) 273–280.
- [3] C. Lagarrigue, J.P. Groby, V. Tournat, O. Dazel, O. Umnova, Absorption of sound by porous layers with embedded periodic arrays of resonant inclusions, J. Acoust. Soc. Am. 134 (6) (2013) 4670.
- [4] X. Li, B. Liu, Q. Wu, Enhanced Low-Frequency Sound Absorption of a Porous Layer Mosaicked with Perforated Resonator, Polymers (Basel) 14 (2) (2022) 233.
- [5] Y. Wang, Y. Wang, J. Xu, H. Yu, C. Zhang, L. Ren, Broadband low-frequency sound absorption by coiled-up space embedded in a porous layer, Appl. Acoust. 182 (2021) 108226.
- [6] Y. Zhou, X. Zhang, Y. Wang, Y. Feng, Dual-band perfect low-frequency acoustic absorption based on metaporous composite, Appl. Phys Express 14 (2021) 094003.
- [7] X.-F. Zhu, S.-K. Lau, Z. Lu, W. Jeon, Broadband low-frequency sound absorption by periodic metamaterial resonators embedded in a porous layer, J. Sound Vib. 461 (2019) 114922.
- [8] Y. Fang, X. Zhang, J. Zhou, Acoustic porous metasurface for excellent sound absorption based on wave manipulation, J. Sound Vib. 434 (2018) 273–283.
- [9] J. Yang, J.S. Lee, Y.Y. Kim, Metaporous layer to overcome the thickness constraint for broadband sound absorption, J. Appl. Phys. 117 (2015) 174903.
- [10] J. Yang, J.S. Lee, Y.Y. Kim, Multiple slow waves in metaporous layers for broadband sound absorption, J. Phys. D Appl. Phys. 50 (2017) 015301.

- [11] H. Zhang, Y. Wang, K. Lu, H. Zhao, D. Yu, J. Wen, SAP-Net: Deep learning to predict sound absorption performance of metaporous materials, *Mater. Des.* 212 (2021) 110156.
- [12] H. Zhang, Y. Wang, H. Zhao, K. Lu, D. Yu, J. Wen, Accelerated topological design of metaporous materials of broadband sound absorption performance by generative adversarial networks, *Mater. Des.* 207 (2021) 109855.
- [13] D.C. Akiwate, M.D. Date, B. Venkatesham, S. Suryakumar, Acoustic Properties of Additive Manufactured Porous Material, *Recent Dev. Acoust.* (2021) 129–138.
- [14] D. Li, D. Chang, B. Liu, Enhanced low- to mid-frequency sound absorption using parallel-arranged perforated plates with extended tubes and porous material, *Appl. Acoust.* 127 (2017) 316–323.
- [15] X. Liu, C. Yu, F. Xin, Gradually perforated porous materials backed with Helmholtz resonant cavity for broadband low-frequency sound absorption, *Compos. Struct.* 263 (2021) 113647.
- [16] X. Yang, K. Peng, X. Shen, X. Zhang, P. Bai, P. Xu, Geometrical and Dimensional Optimization of Sound Absorbing Porous Copper with Cavity, *Mater. Des.* 131 (2017) 297–306.
- [17] M. Toyoda, K. Sakagami, M. Okano, T. Okuzono, E. Toyoda, Improved sound absorption performance of three-dimensional MPP space sound absorbers by filling with porous materials, *Appl. Acoust.* 116 (2017) 311–316.
- [18] Z. Liu, J. Zhan, M. Fard, J.L. Davy, Acoustic measurement of a 3D printed micro-perforated panel combined with a porous material, *Measurement* 104 (2017) 233–236.
- [19] X. Shen, P. Bai, X. Yang, X. Zhang, S. To, Low Frequency Sound Absorption by Optimal Combination Structure of Porous Metal and Microperforated Panel, *Appl. Sci.* 9 (7) (2019) 1507.
- [20] F. Xin, X. Ma, X. Liu, C. Zhang, A multiscale theoretical approach for the sound absorption of slit-perforated double porosity materials, *Compos. Struct.* 223 (2019) 110919.
- [21] X. Ma, X. Liu, F. Xin, Sound absorption performance of gradually slit-perforated double-porosity materials, *Chin. J. Acoust.* 40 (1) (2021) 1–17.
- [22] K. Attenborough, Analytical Approximations for Sub Wavelength Sound Absorption by Porous Layers with Labyrinthine Slit Perforations, *Appl. Sci.* 11 (8) (2021) 3299.
- [23] X. Liu, M. Duan, M. Liu, F. Xin, C. Zhang, Acoustic labyrinthine porous metamaterials for subwavelength low-frequency sound absorption, *J. Appl. Phys.* 129 (2021) 195103.
- [24] N. Atalla, R. Panneton, F.C. Sgard, X. Olny, Acoustic Absorption of Macro-Perforated Porous Materials, *J. Sound Vib.* 243 (4) (2001) 659–678.
- [25] X. Liu, F. Xin, C. Zhang, High-temperature effect on the sound absorption of cylindrically perforated porous materials, *J. Appl. Phys.* 130 (2021) 105101.
- [26] Q. Liu, X. Liu, C. Zhang, F. Xin, A novel multiscale porous composite structure for sound absorption enhancement, *Compos. Struct.* 276 (2021) 114456.
- [27] Q. Liu, X. Liu, C. Zhang, F. Xin, High-Temperature and Low-Frequency Acoustic Energy Absorption by a Novel Porous Metamaterial Structure, *Acta Mech. Solida Sin.* 34 (6) (2021) 872–883.
- [28] F. Sun, H. Chen, J. Wu, K. Feng, Sound absorbing characteristics of fibrous metal materials at high temperatures, *Appl. Acoust.* 71 (3) (2010) 221–235.
- [29] J.H. Wu, Z.P. Hu, H. Zhou, Sound absorbing property of porous metal materials with high temperature and high sound pressure by turbulence analogy, *J. Appl. Phys.* 113 (2013) 194905.
- [30] S. Ren, F. Xin, T.J. Lu, C. Zhang, A semi-analytical model for the influence of temperature on sound propagation in sintered metal fiber materials, *Mater. Des.* 134 (2017) 513–522.
- [31] X. Olny, C. Boutin, Acoustic wave propagation in double porosity media, *J. Acoust. Soc. Am.* 114 (1) (2003) 73–89.
- [32] J.F. Allard, N. Atalla, *Propagation of Sound in Porous Media: Modelling Sound Absorbing Materials*, Second Edition, John Wiley & Sons, 2009.
- [33] Y. Tang, F. Xin, T.J. Lu, Sound absorption of micro-perforated sandwich panel with honeycomb-corrugation hybrid core at high temperatures, *Compos. Struct.* 226 (2019) 111285.
- [34] D.R.A. Christie, Measurement of acoustic properties of a sound absorbing material at high-temperatures, *J. Sound Vib.* 46 (3) (1976) 347–355.
- [35] J.P. Abulencia, L. Theodore, *Fluid Flow for the Practicing Chemical Engineer: Ideal Gas Law*, John Wiley & Sons, 2009, pp. 109–119.
- [36] P.T. Williams, R. Kirby, C. Malecki, J. Hill, Measurement of the bulk acoustic properties of fibrous materials at high temperatures, *Appl. Acoust.* 77 (2014) 29–36.
- [37] Y.S. Touloukian, R.K. Kirby, R.E. Taylor, P.D. Desai, *Thermophysical Properties of Matter*, The TPRC Data series Vol. 12 Thermal Expansion-Metallic Elements and Alloys (IFI/Plenum, New York, 1975).
- [38] D.H. Kim, B.Y. Yu, P.R. Cha, W.Y. Yoon, J.Y. Byun, S.H. Kim, A study on FeCrAl foam as effective catalyst support under thermal and mechanical stresses, *Surf. Coat. Technol.* 209 (2012) 169–176.
- [39] Y. Fang, X. Zhang, J. Zhou, Sound transmission through an acoustic porous metasurface with periodic structures, *Appl. Phys. Lett.* 110 (2017) 171904.